Sensors & Actuators: B. Chemical 424 (2025) 136881

Contents lists available at ScienceDirect

Sensors and Actuators: B. Chemical

journal homepage: www.elsevier.com/locate/snb

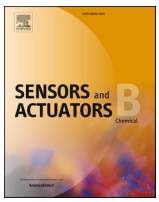

A paper-based analytical device for the on-site multiplexed monitoring of soil nutrients extracted with a cafetière

Pablo Giménez-Gómez [a,*], Nicolina Priem [a], Samantha Richardson [b], Nicole Pamme [a,b,**]

[a] Department of Materials and Environmental Chemistry, Stockholm University, Stockholm 106 91, Sweden
[b] School of Natural Sciences, University of Hull, Hull, United Kingdom

ARTICLE INFO

Keywords:
Paper-based analytical device
Multiplexed soil nutrient monitoring
In-the-field agricultural control
Phosphate
Nitrate and pH detection
Cafetière-based soil extraction

ABSTRACT

Sustainable agricultural production has the aim to maximise the yield and quality of harvests. For that, farmers need to monitor nutrient levels within soils to apply fertilizers accordingly and to prevent land degradation and soil exhaustion. Current methods involve time-consuming sampling and transport to a laboratory; and most farmers do not have the resources to measure frequently at multiple locations, limiting their sustainable production. In order to address this challenge, a paper-based analytical device (PAD) for the multiplexed detection of soil nutrients, *i.e.* phosphate, nitrate and pH, extracted with a cafetière-based method, is developed in this work. The compact and easy-to-use platform enables an accurate soil analysis in less than 20 min; 3 min for extraction and 15 min for readout. Two detection channels for nitrate and phosphate analysis, and one circular detection area for pH, including the selective reagents to each analyte, are defined within the PAD. Upon contact with the specific nutrients, the platform produces a colorimetric response that is easily readable by naked eye and smartphone camera. The detection reactions were optimized in the range 1 – 22.5 mg L^{-1}, 10 –100 mg L^{-1} and 5.0 – 8.5 for phosphate, nitrate and pH, respectively, in agreement with the relevant levels in soils. The volume of water, the number of pushes of the plunger, the extraction time and the mass of soil were also optimized for the nutrient extraction method with the cafetière. The optimal workflow was validated with commercial soils and compared with the conventional UV-Vis method and the labels from the soil package, showing excellent agreement. This paper-based platform provides the possibility of a cheap, sensitive and specific monitoring of soil nutrients by minimally trained operators, such as farmers, enabling in-the-field analyses of multiple key soil nutrients in resource-limited settings and therefore addressing the challenge of routine monitoring for sustainable agriculture.

1. Introduction

Population rise is increasing the demand of food production [1], resulting in a higher use of fertilizers (*e.g.*, nutrients) to try to improve soil productivity [2]. Nevertheless, excessive use of synthetic fertilizers provokes a negative impact both on the environment and the sustainability of agricultural activity [3–5]. Nitrate and phosphate, with optimal levels of 60 – 150 mg L^{-1} and 40 – 60 mg L^{-1}, respectively, are two of the essential macronutrients in soil because of their influence on plant growth [6,7]. Moreover, the soil pH has a high influence on these nutrients because acidity/alkalinity affects their release, complexation and availability [8]. Most soils have a pH in the range from 3 to 9, but the generally accepted optimal range is from 5 to 7.5 [9]. Over-fertilisation causes saturation of nutrients in plants, provoking an enrichment of the soil with nutrients which affects its fertility, and the release of these nutrients to the surrounding areas with a high negative environmental impact (*e.g.*, eutrophication of waters or greenhouse gas emissions) [10–15]. Therefore, a balanced supplementation of nutrients is fundamental to optimize soil management. Doing this results in a sustainable agricultural production, mitigating the environmental impact of food production [16–18]. To achieve it, soil monitoring is required to know the temporal and spatial evolution of nutrient levels and acidity, allowing mapping of the soil composition and thus adapting the fertilizer application accordingly [19,20].

Standard methods to analyze nutrients in soils are laborious, involving extensive sample preparation (*i.e.*, extraction, dilution,

* Corresponding author.
** Corresponding author at: Department of Materials and Environmental Chemistry, Stockholm University, Stockholm 106 91, Sweden.
E-mail addresses: pablo.gimenez-gomez@mmk.su.se (P. Giménez-Gómez), nicole.pamme@mmk.su.se (N. Pamme).

https://doi.org/10.1016/j.snb.2024.136881
Received 18 July 2024; Received in revised form 2 October 2024; Accepted 30 October 2024
Available online 8 November 2024

complexation) and long analysis times (*i.e.*, spectrophotometric readout), making then ineffective for on-site analysis [21,22]. Colorimetric and electrochemical methods have been also proposed [23]. Colorimetric tests show a good accuracy and a fast response for phosphate, nitrate and pH, but they need a spectrophotometer to read the nutrient concentration, limiting their portability and increasing their cost [24–29]. Other approaches using a digital camera as colorimetric detector with consistent results have been published [30–32], but the set-ups for preparing and read the value are difficult to use by minimally trained operators (*e.g.*, farmers). Regarding electrochemical sensors, most of them are based on ion-selective electrodes (ISE) working by potentiometry [33–40] or cyclic voltammetry [41,42]. They are very selective and reproducible, but they usually require a complex electronical set-up. Potentiometric and optical portable kits for on-field detection can be also found on the market for nitrate, phosphate and pH [43–46]. Nevertheless, they are expensive, require semi-skilled operators or use aggressive reagents, resulting in a no real alternative for members of the general public.

As an alternative to standard methods, microfluidic-based systems can perform rapid assays at the point-of-need [47]. The integration of both opto-colorimetric and electrochemical readouts into glass, silicon or polymer-based microfluidics for phosphate or nitrate detection has been explored [48–52], but they are expensive to fabricate or require power suppliers for pumping and detecting, restricting their use in resource-limited settings. Due of these drawbacks, paper-based analytical devices (PADs) arise as a more convenient approach because they constitute a good compromise between high performance, low cost, and simplicity [53]. Cellulose is inexpensive, lightweight, biodegradable, abundant, and allows passive fluid manipulation through capillary action due to its hydrophilicity and porosity. Moreover, PADs are easy to operate by untrained users, enabling a more frequent quantification with expanded geographical coverage. There are some works in the literature describing PADs for nitrate [54–56] and phosphate [57,58]. A few articles have also been published using multiplexed colorimetric PADs for phosphate and nitrate detection from water samples [59,60]. Nitrate detection in PADs is usually based on the reduction of nitrate to nitrite by a reductant (*i.e.*, Zn), followed by the nitrite detection with the Griess reaction [61]. Phosphate in turn can be detected by the formation of the phosphomolybdenum blue (PMB) complex [62]. The PADs incorporate reaction areas loaded with these color changing reagents that produce a change in color intensity depending on the concentration of the specific nutrient. Then, the color can be recorded with a smartphone camera and an image processing program is used to quantify the concentration according to its intensity. Although they are a good alternative to more complicated conventional methods, the intensity-based readout could be complicated to interpret by the general public and could produce some interferences depending of the light conditions during the image recording. Because of this, colorimetric distance-based paper analytical devices (dPADs) arose as an alternative to intensity-based PADs. In the dPAD, a channel is defined on the paper, which is modified with the colorimetric reagents reacting with the analyte of interest. When the sample containing the analyte flows through the channel, the colorimetric reaction occurs until the analyte is consumed. Then, the length of the color is correlated to the concentration of the analyte [63]. The distance-based readout is easier to interpret by non-qualified personnel, and the distance could be also read using just a ruler, resulting in a real alternative for minimally trained operators located in resource limited settings (*i.e.*, farmers). Whilst some dPADs can be found in the literature detecting some analytes in water, to the best of our knowledge, phosphate and nitrate have not yet been described. Moreover, there are no publications either using PADs for simultaneous detection of these nutrients from soils, because their extraction is complex, involving processes such as sedimentation or filtering [64].

Here, in order to address this challenge, we report the development of a rapid and easy-to-use method for on-site monitoring phosphate and nitrate in soil by integrating two dPADs with a nutrient extraction method using a cafetière. In order to complete the collected information from soils, and intensity-based PAD for pH is also integrated in the multiplexed PAD. The extraction from soil is carried out by mixing a soil sample with deionized water (DIW) in a cafetière, pouring the resulting solution into a beaker into which the PAD is dipped. The multiplexed PAD includes two reaction channels for phosphate and nitrate detection, and a circular zone for pH. The phosphomolybdenum blue reaction [58] and the combined zinc reduction and Griess reaction [65] were adapted to a distance format for the phosphate and the nitrate detection, respectively. For pH, chlorophenol red indicator [66] was used to modify the intensity-based detection area. This multiplexed PAD design integrating two dPADs for nitrate and phosphate allows a much simpler readout of the soil's composition compared to those based on intensity response, allowing its use by unqualified personnel in limited access environments, such as farms or crop fields. The integration of the multiplexed PAD with the cafetière-based work-flow for nutrient extraction from soils, results in a cheap and easy-to-use method for the decentralized extraction and analysis of soils nutrient, overcoming the limitations of current methods. The extraction method was optimized in terms of mass of soil, volume of water, number of times for pressing the plunger and the soaking time. In the multiplexed PAD, the concentrations and volumes of the reagents involved in the color-based detections were optimized, and the analytical response of the PAD was studied in terms of linear range, sensitivity, selectivity, limit of detection, working stability and cross contamination. Finally, the optimized protocol was validated with four different commercial soils and compared for PADs, UV/vis measurements and the labels on the soil packages.

2. Experimental

2.1. Reagents and solutions

For the nitrate detection, citric acid (ACS reagent, ≥99.5 %), N-(1-Naphthyl)ethylenediamine dihydrochloride (NED, ACS reagent, >98 %), potassium nitrate (ACS reagent, ≥99.0 %) and sodium nitrite (≥99.5 %) were purchased from Sigma-Aldrich (Stockholm, Sweden). Zinc powder (7.5 micron, 98.8 %) and sulphanilamide (98 %) were purchased from GoodFellow (Hamburg, Germany) and ThermoFisher-Scientific (Stockholm, Sweden), respectively. For the phosphate analysis, ammonium molybdate (para) tetrahydrate (99 %), ammonium potassium tartrate hydrate (98 %), L(+)-Ascorbic acid (99 %) and sodium phosphate (monobasic, anhydrous, 99 %) were purchased from ThermoFisherScientific (Stockholm, Sweden). p-Toluenesulfonic acid (TsOH, ACS reagent, ≥98.5 %) was obtained from Sigma-Aldrich (Stockholm, Sweden). For pH measurements, hydrochloric acid, sodium hydroxide, poly-diallyl-dimethyl-ammonium chloride solution (PDADMAC, 20 wt% in H_2O), chlorophenol red indicator and phosphate buffered saline (PBS, tablets, pH 7.4) were sourced from Sigma-Aldrich (Stockholm, Sweden). The interference tests were performed by using sodium nitrate (≥99.0 %), sodium sulphate (≥99.0 %), potassium nitrate (≥99.0 %) and calcium sulphate (analytical grade) from Sigma-Aldrich (Stockholm, Sweden), sodium phosphate (monobasic, anhydrous, 99 %) from ThermoFisherScientific (Stockholm, Sweden), and magnesium sulphate anhydrous (analytical grade) from Mallinckrodt (Dublin, Ireland). Unless otherwise stated, all solutions were prepared with DIW (Milli-Q® IQ 7000 Ultrapure Water System, Sigma-Aldrich, Stockholm, Sweden).

2.2. Equipment

The wax-based hydrophobic barriers defining the detection channels and circles on the paper substrate were printed with a ColorQube ™ 8570 (Xerox, Connecticut, USA) printer. A Saturn 3i A4 laminator (Fellowes, Illinois, USA) was used for melting the wax through the paper thickness and to laminate the PADs. The pH was measured with a digital

pH-meter (Jenway 3510, Cole-Parmer, Illinois, USA) equipped with a glass-bodied pH electrode (Jenway 924 005, Cole-Parmer, Illinois, USA). UV-Vis analysis was performed with a Lightwave 3 and 3+ UV-Vis spectrometer (Harvard Bioscience, Massachusetts, USA). A cafetière (French coffee maker, 1 L, IKEA, Stockholm, Sweden) was utilized to extract the nutrients from the soil samples.

2.3. Design and fabrication of the paper-based fluidic device

A 55 mm height × 48 mm width × 460 μm thickness PAD was formed from Whatman Grade 4 filter paper (particle retention 25 μm, nominal thickness 210 μm, nominal basis weight 92 g m^{-2}, nominal ash content ≤ 0.06 %) (Cytiva, Uppsala, Sweden), which was sandwiched between two 125 μm-thick layers of polyethylene terephthalate laminating pouch (PET, MattPouch, Conrad Electronic SE, Hirschau, Germany). AutoCAD 2023 (Autodesk, California, USA) was used to design the PAD, which was printed with the Xerox ColourCube printer loaded with wax cartridges on the paper substrate. Three different colored wax areas, *i.e.*, green, red and blue, defined the detection areas for the nitrate, phosphate and pH, respectively (Fig. 1**a**). For both the nitrate and the phosphate, a channel area of 40 mm × 6 mm was left free of wax. For the pH, a wax-free circle of 11 mm diameter was also defined. Another identical circle was defined next to the first one, in such a way that when folded they both overlapped. Afterwards, the wax on the paper was melted at 125 °C with the laminator (Fig. 1**b**), defining a hydrophobic wax barrier throughout the thickness of the paper. Then, the hydrophilic channels and the circle most to the right were chemically modified by drop casting, and the modified circle was folded over the unmodified circle (Fig. 1**c**) and dried in air for 1 h. To protect the reagents while storing the PAD, the device was laminated between two transparent PET sheets at 125 °C (Fig. 1**d**). The finished PAD is shown in Fig. 1**e**.

2.4. Fabrication of the detection areas

The detection areas for each parameter were optimized separately prior to their integration into the multiplexed PAD. For the nitrate and phosphate, two dPADs were used. The chemically modified detection channels specifically react with phosphate or nitrate. The bottom part of the channel is cut off (Fig. S1a, **part i**) to open the channel (Fig. S1a, **part ii**) before dipping it in the sample (Fig. S1a, **part iii**), and the channel is filled with the solution containing phosphate or nitrate. The sample reacts with the deposited reagents in the detection channel, producing a change of color, the length of which depends on the concentration of the nutrient in the sample (Fig. S1a, **part iv**). The length of

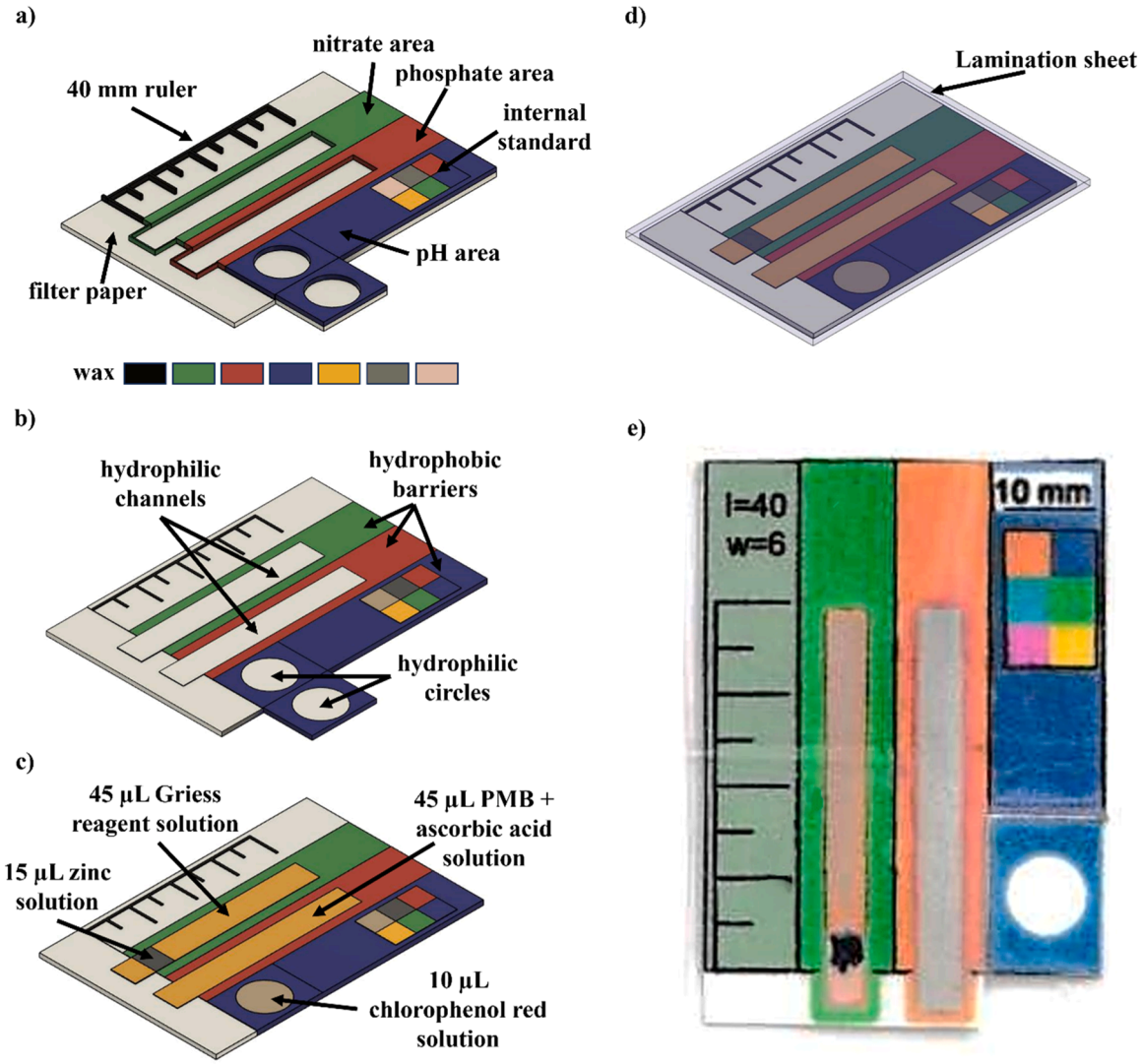

Fig. 1. PAD fabrication process. a) Wax layers printed on filter-paper. b) Hydrophobic barriers and hydrophilic areas created by melting the wax through the paper. c) Modification of the detection areas with the specific chemicals by drop casting. d) Lamination of the PAD at 125 °C. e) Image of the finished PAD for the simultaneous detection of nitrate, phosphate and pH.

the change of color can be measured with the integrated ruler on the dPAD or with the help of a software (ImageJ, National Institutes of Health (NIH), Maryland, USA) after photographing the dPAD (Fig. S1b). In the case of the pH quantification, a colorimetric PAD was fabricated by defining a reaction circle which was chemically modified to specifically change of color depending of the pH of the solution. A cross was cut with a scalpel on the laminated sheet covering the detection circle (Fig. S2a**, part i**), and the PAD was dipped in a solution for filling the circle (Fig. S2a**, part ii**). Then, a color change occurs, the intensity of which depends on the solution pH (Fig. S2a**, part iii**). The printed internal standard allows to remove the effects from the lighting conditions and camera-to-camera differences during image analysis. Finally, the photographed or scanned image of the PAD was be analysed with the ImageJ software to quantify the pH of the sample (Fig. S2b).

2.5. Optimization of the detection scheme

For nitrate, the detection channel was chemically modified with a suspension of a reductant (zinc) to enable reduction of nitrate to nitrite as well as reagents for the colorimetric Griess reaction to detect nitrite [67] (Fig. S3). The optimized channel design obtaining the best distance-based colorimetric detection for nitrate on a dPAD was 40 mm in length and 6 mm in width. The optimal design was modified with the optimized reagent solutions, *i.e.* the first 0.5 cm modified with 15 μL of 50 mg mL^{-1} zinc suspension and the remainder of the channel with 45 μL of Griess reagent solution containing 100 mM ammonium sulphanilamide, 400 mM acid citric and 3 mM NED. The optimal design and reagent solution were used to study the linear range, sensitivity and limit of detection (LOD) of the dPAD in DIW solutions with nitrate concentrations from 0 mg L^{-1} to 100 mg L^{-1}.

In the case of phosphate, the detection is based on the colorimetric PMB reaction [68] (Fig. S4). The method applied by Richardson *et al.* in a color intensity-based PAD [58] was optimized to adapt the method to a distance-based approach in this work. The dimensions of the detection channel were also optimized (*i.e.,* 40 mm length and 6 mm width) to obtain the best signal for phosphate detection. The optimal phosphate dPAD design modified with the optimized reagent solutions, *i.e.*, 45 μL of 0.01 M ascorbic acid, 7.5 M TsOH, 0.01 M ammonium molybdate and 6 mM antimony tartrate, was used to fully characterize its response in solutions with phosphate concentrations from 0 mg L^{-1} to 22.5 mg L^{-1}.

For both the phosphate and nitrate dPADs, interference tests were performed in presence of the most common macronutrients considering the concentration ratio of each one in relation to the nitrate and phosphate in soils (Table S1). Additional interference tests were also performed for nitrate and phosphate by adjusting the pH (from 5 to 8) of standard solutions to investigate its influence on the produced color in the detection channels.

The long-life working stability of the phosphate and nitrate dPADs was studied by preparing 200 nitrate dPADs and 200 phosphate dPADs, and placing 100 of each one in the fridge at 4 °C and 100 in a cupboard at room temperature. During three weeks, a set of 18 dPADs for each nutrient, *i.e.*, nine dPADs from the fridge and 9 dPADs from the cupboard, was tested twice peer week. Ten mg L^{-1}, 50 mg L^{-1}, and 100 mg L^{-1} of nitrate solutions and 2.5 mg L^{-1}, 10 mg L^{-1}, 25 mg L^{-1} of phosphate solutions, were used to test the nitrate and phosphate dPADs, respectively.

For the pH measurements, the pH indicator chlorophenol red was used (Fig. S5) [69]. An optimized PBS solution at pH 3.5 with 0.1 mg mL^{-1} chlorophenol red and 10 wt% PDADMAC was used as reagent solution. PDADMAC is a cationic polymer used as binding agent to prevent washout of the reagents in the reaction area to the sample solution [70]. A wax-free circle of 11 mm diameter was modified by pipetting 10 μL of the indicator solution and air dried for 1 h. Then, the colorimetric response (*i.e.,* linear range, sensitivity) of the circles in contact with PBS solutions with a pH of 5.5 and 8.5, was studied

The three optimized single analyte PADs for nitrate, phosphate and pH were integrated into a single multiplexed PAD shown in Fig. 1. The multiplexed PAD was characterized in terms of cross contamination between the integrated detection zones, by keeping constant two of the parameters and changing the third (Table S2). The required time for filling the integrated nitrate and phosphate detection channels, as well as the required time to achieve a constant color in the pH circle, were checked in a water solution containing 20 mg L^{-1} of phosphate and 50 mg L^{-1} of nitrate at pH 7. The deviation of the response for each PAD over time was also analyzed at different time points over 60 min in the same aqueous solution.

2.6. Extraction of nutrients from soils and workflow for quantification of nutrients

A cafetière-based method is developed here to extract the soluble nutrients from soils samples (Fig. 2**a**). Soil and water are added to the coffee maker glass (Fig. 2**a, part i**). Afterwards, the plunger that holds the metal mesh filter is introduced into the coffee maker (Fig. 2**a, part ii**) and moved up and down to properly mix the soil and water and transfer the nutrients from the soil to the water (Fig. 2**a, part iii**). The mixed solution is left to sit for some minutes to stabilise itself, and then the plunger is pressed down to separate the soil from the water (Fig. 2**a, part iv**). For measuring the transferred nutrient from the soil to the water, firstly the multiplexed PAD is prepared. The proposed design for the multiplexed PAD allows to minimize human error during its manipulation. Most of the described multiplexed PADs in the literature involve some pipetting or precise manipulation of the PAD and the sample before the analysis [71], limiting their use by non-trained personnel in real circumstances. In the design proposed here, the user only has to cut off the 5-mm bottom part of the PAD to open the channels of the phosphate and nitrate, and to cut a cross on the back of the pH PAD with a scalpel (Fig. 2**b, part i**). Then, a volume of the water containing the soluble nutrients extracted from the soil is transferred from the cafetière to a container (Fig. 2**b, part ii**), and the multiplexed PAD is just dipped in a volume of solution to expose the bottom part of the opened channels to the sample and to dip the detection circle for the pH in the solution (Fig. 2**b, part iii**). After 15 min, the detection areas are fully filled with the sample solution, giving a colorimetric response depending on the nutrient levels in the sample (Fig. 2**b, part iv**). Finally, the length of the color change for both the phosphate and nitrate channels is measured with the ruler integrated in the PAD, or taking a photograph or scanning the PAD to measure the distance with the ImageJ software. For the circle, a scanned or photographed image of the PAD is analysed with the Image J software to quantify the pH value of the sample (Fig. 2**b, part v**).

2.7. Analysis of soil samples

Firstly, the extraction protocol described above with the cafetière was optimized in terms of the mass of soil, volume of water, number of times the plunger was pressed and the time for letting the soil sample soak in the water (Table S3). A commercial planting soil with a concentration of phosphate of 20 mg L^{-1} and a concentration of nitrate of 80 mg L^{-1} was used in this study.

The optimized workflow was then tested for four different commercial soils (Table S4), with labelled values in the range 2 − 7 mg L^{-1}, 56 −85 mg L^{-1} and 5 – 7 for phosphate, nitrate and pH, respectively. The quantified values of phosphate and nitrate were also compared with those obtained from UV-Vis measurements (Fig. S9 **and** Fig. S7), which was used as a gold standard method to validate the results. For the pH detection, the calculated pH of each sample was compared to the pH obtained using a pH-meter. All the samples were measured in triplicate, *i.e.* three multiplexed PADs were fabricated under the same conditions for each analysis (n = 3). Finally, the results from the multiplexed PADs were also compared with the labelled values in the soil packages.

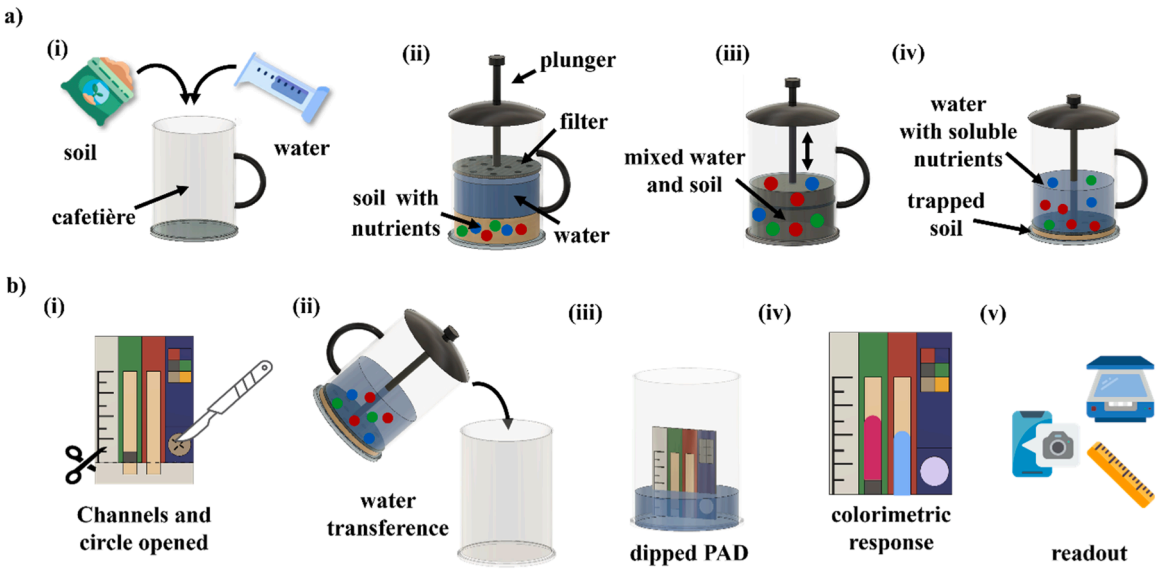

Fig. 2. Procedure for the determination of nutrients in soils. a) Steps followed for nutrients extraction from soils: (i) addition of water and soil; (ii) insertion of the plunger; (iii) mixing of soil and water with the plunger; and (iv) stabilization of the extracted nutrients. b) Steps to measure the extracted nutrients: (i) opening of the reaction areas; (ii) transfer of extracted nutrients to a container; (iii) dipping the PAD in the solution; (iv) colorimetric response of the PAD; and (v) readout.

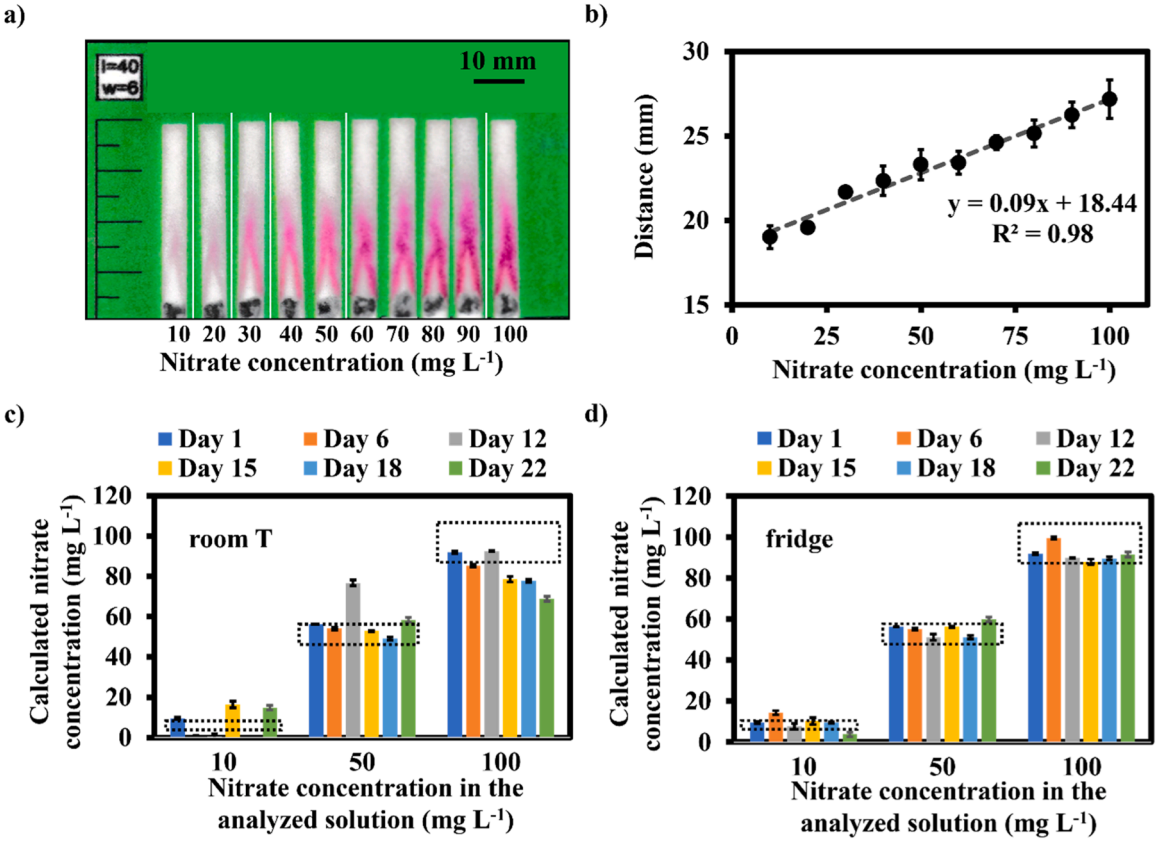

Fig. 3. Analytical response of the dPAD for nitrate detection. a) Photographs of the detection channels used for measuring nitrate in the range from 10 mg L^{-1} to 100 mg L^{-1}. b) Calibration plot representing the distance measured for each dPAD versus the concentration of the analyzed solution. c) Calculated nitrate concentration with dPADs stored at room temperature over a period of three weeks. d) Calculated nitrate concentration with dPADs stored in the fridge over a period of three weeks. Dashed rectangles in the graph define an interval of error of 10 % with respect to expected nitrate concentration in the sample (90 – 110 mg L^{-1}, 45 – 55 mg L^{-1} and 11 – 9 mg L^{-1} for the samples containing 100 mg L^{-1}, 50 mg L^{-1} and 10 mg L^{-1}, respectively). Errors represent the standard deviation for five replicates (n = 5).

3. Results and discussion

3.1. Optimization of the nitrate dPAD

Initially, the design for the nitrate dPAD (Fig. S8) was studied. Volumes of reagent solution between 15 μL and 45 μL were pipetted on the channels and air dried for 1 h. A 50 mg mL^{-1} zinc suspension in DIW was used for reduction. The Griess reagent solution contained 300 mM citric acid, 50 mM sulphanilamide and 6 mM NED. The produced dPADs were dipped in a 30 mg L^{-1} nitrate solution, and the results were compared in terms of the obtained distance and the clarity of the color change in the channel (Fig. S9). The design immobilizing 15 μL of 50 mg mL^{-1} zinc suspension at the bottom 0.5 cm of the channel and 45 μL of the Griess reagent in the rest of the channel (Fig. S9, **design 1**) was selected as the best because it showed a clearer and a darker pink color in comparison to the others.

Then, the optimal design was used to optimize the Griess reagent solution concentration, varying the concentrations of sulphanilamide, NED and citric acid (Table S5). The produced dPADs for each concentration were analyzed in DIW solutions with 30 mg L^{-1} and 60 mg L^{-1}, and the results were compared in terms of the obtained distance and the clarity of the color change in the channel. From the results is can be concluded that the optimal Griess solution should contain 400 mM citric acid (Fig. S10), 100 mM sulphanilamide (Figs. S11), and 3 mM NED (Fig. S12) for obtaining a bright and consistent color line in the presence of nitrate.

The selected optimal design and reagent solutions, *i.e.* a 40 mm long and 6 mm wide channel, with the first 0.5 cm modified with 15 μL of 50 mg mL^{-1} zinc suspension and the remainder of the channel with 45 μL of Griess reagent solution containing 100 mM ammonium sulphanilamide, 400 mM acid citric and 3 mM NED, were utilized to analyze solutions with different concentrations of nitrate. The length of the pink color in the detection channel increased for increasing concentrations of nitrate, as expected (Fig. 3**a**). The length was defined by measuring the distance from the bottom part of the channel to the top of the pink color. Although the shape of the top part of the pink color is somewhat irregular, the contrast of the pink color with the channel background color is sufficient to delimit the top part of the pink color. The sensitivity of the calibration plot of the measured distance versus the nitrate concentration was 0.092 ± 0.001 mm mg^{-1} L, with a linear range from 10 mg L^{-1} to 100 mg L^{-1} and a coefficient of regression of 0.98 (Fig. 3**b**). The calculated LOD according to the 3σ IUPAC criterion was 9.53 ± 0.09 mg L^{-1}. The reproducibility of the dPAD fabrication was studied by preparing five different dPADs under the same conditions, obtaining a relative standard deviation lower than 8 % for all the dPADs.

The potential applicability of the nitrate dPAD in soil samples was tested by measuring the response of the dPAD in a solution containing nitrate and the maximum expected relative concentration of the most common macronutrients present in soils. The results (Fig. S13) show that the measured length produced change of the color produced in the detection channel does not fluctuate in the presence of these macronutrients, meaning that the presence of these other macronutrients does not significantly interfere with the nitrate analysis.

Finally, long-term working stability tests were performed for the nitrate dPADs stored in the fridge and at room temperature in dark conditions. For those dPADs stored in the fridge (Fig. 3**c**), the calculated concentration of nitrate in the first 18 days was 10.3 ± 2.5 mg L^{-1} for the solution containing 10 mg L^{-1} of nitrate, meaning that there was a slight overestimation error of 3 %. For day 22, the calculated concentration dropped to 3.8 ± 1.2 mg L^{-1}, resulting in an underestimation of more than 40 %. For the 50 mg L^{-1} nitrate solutions, the average calculated concentration for the three weeks was 54.9 ± 3.3 mg L^{-1}, resulting in an overestimation error of 9 %. In the case of the solution containing 100 mg L^{-1} of nitrate, the calculated concentration was 91.7 ± 4.1 mg L^{-1} (*i.e.*, an underestimation error of 9 %). The analyses performed with the dPADs at room temperature resulted in a calculated concentration of 4.9 ± 10.3 mg L^{-1} for those in presence of 10 mg L^{-1} of nitrate (*i.e.*, underestimation error of 51 %), 57.9 ± 9.7 mg L^{-1} for those in presence of 50 mg L^{-1} of nitrate (i.e., overestimation error of 16 %) and 82.4 ± 9.2 mg L^{-1} for those in the presence of 100 mg L^{-1} of nitrate (*i.e.*, underestimation error of 18 %). These results demonstrate that the stored dPADs at room temperature can only be used the same day that they are fabricated, especially for lower concentrations, probably because the sulphanilamide decomposes under these conditions [72]. In case of the dPADs stored in the fridge, the stability of the reagents significatively improved during the first 18 days, and then suddenly decreased for lower concentrations. Therefore, nitrate dPAD can be used over 18 days after their fabrication with a high accuracy in all the studied range if they are stored in the fridge at 4°C.

3.2. Optimization of the phosphate dPAD

The conditions applied by Richardson *et al.* [58] were optimized to transfer the phosphate detection with the PMB reaction from a color intensity-based circle to a distance-based format with a channel. Richardson *et al.* used 2 M TsOH to provide the acidity needed to minimise the auto-reduction of the 0.01 M ammonium molybdate in the first step of the reaction. Six mM of antimony tartrate was also added to improve the rate of reduction and to avoid the necessity to heat the reaction [73]. Finally, 0.01 M of ascorbic acid was used as reductant in the second step of the reaction. Here, the PMB reagent and ascorbic acid solutions were optimized in order to transfer the phosphate detection with the PMB reaction to a distance-based format. The effect of varying the concentration of TsOH, ammonium molybdate, antimony tartrate and ascorbic acid was studied (Table S6). A detection channel of 40 mm length and 3 mm width was used during this optimization (Fig. S14, **design 1**). Thirty μl of the reagent solution, with a ratio 1:2 between the PMB reagent and the ascorbic acid solution was pipetted into the channel and air dried for 1 h. The produced dPADs were analyzed in DIW solutions with a phosphate concentration in the range 0 mg L^{-1}– 10 mg L^{-1}, and the results shows the effect in the response of the concentration of the ascorbic acid (Fig. S15), the ammonium molybdate (Fig. S16) and the TsOH (Fig. S17). The clearest signal preventing the auto-coloring of the channel was obtained for a reagent solution containing 0.01 M ascorbic acid, 0.01 M ammonium molybdate, 6 mM antimony tartrate and 7.5 M TsOH, which was selected as optimal for the next assays.

The optimal reagent solution was then used to optimize the width of the detection channel (*i.e.*, 4 mm or 6 mm, Fig. S14) in a 10 mg L^{-1} phosphate solution. The results show that the narrower channel (Fig. S18a) produced a three times shorter color change in comparison to the wider channel (Fig. S18b). Moreover, the color was more evident for the 6 mm width channel, resulting in an easier to use dPAD to quantify phosphate.

The optimal phosphate dPAD, *i.e.*, a channel of 40 mm length and 6 mm width modified with 45 μL of 0.01 M ascorbic acid, 7.5 M TsOH, 0.01 M ammonium molybdate and 6 mM antimony tartrate, was fully characterized in solutions with phosphate concentrations from 0 mg L^{-1} to 22.5 mg L^{-1}. The length of the colorimetric response was defined by measuring the distance from the bottom part of the channel to the top of the blue-grey colored channel, whose contrast with the color background does not give rise to errors. As expected, the length of the produced blue-grey color in the detection channel increases for increasing concentrations of phosphate (Fig. 4**a**), with a sensitivity of 0.23 ± 0.02 mm mg^{-1} L, in a linear range from 1.0 mg L^{-1} to 22.5 mg L^{-1} and a coefficient of regression of 0.97 (Fig. 4**b**). The LOD (3σ IUPAC criterion) was 2.82 ± 0.06 mg L^{-1}. The reproducibility of the dPAD fabrication (n = 5) presented a relative standard deviation lower than 6 % for all cases.

The response of the phosphate dPAD was analyzed in the presence of the most common macronutrients in soils. The results (Fig. S19) show that the signal for phosphate does not change significatively in presence

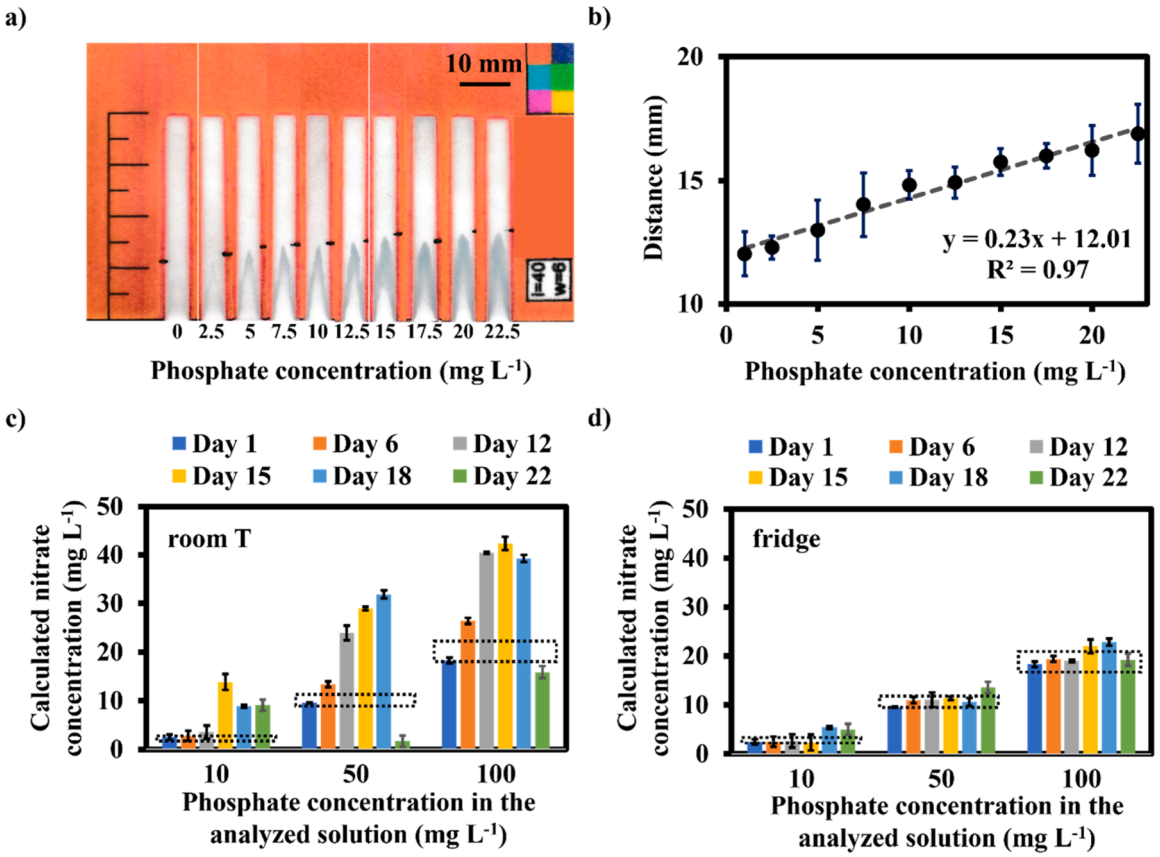

Fig. 4. Analytical response of the dPAD for phosphate detection. a) Photographs of the detection channels used for measuring phosphate in the range from 0.0 mg L^{-1} to 22.5 mg L^{-1}. b) Calibration plot representing the distance measured for each dPAD versus the concentration. c) Calculated phosphate concentrations with dPADs stored at room temperature over a period of three weeks. d) Calculated phosphate concentrations with dPADs stored in the fridge over a period of three weeks. Dashed rectangles in the graph define an interval of error of 10 % with respect to the expected nitrate concentration in the sample (18 – 22 mg L^{-1}, 9 – 11 mg L^{-1} and 2.25 – 2.75 mg L^{-1} for the samples containing 20 mg L^{-1}, 10 mg L^{-1} and 2.5 mg L^{-1}, respectively). Errors represent the standard deviation for five replicates (n = 5).

of these other macronutrients, therefore, the specificity of the developed dPAD for phosphate in soil is validated.

The long-term working stability of the optimized phosphate dPAD was also checked during three weeks by storing two sets of dPADs in the fridge at 4°C and at room temperature in dark conditions. The results from the dPADs stored at room temperature (Fig. 4**c**) for the first three days were 2.6 ± 0.2 mg L^{-1}, 11.5 ± 2.7 mg L^{-1} and 22.3 ± 5.8 mg L^{-1}, with an overestimation of 4 %, 15 % and 12 % in comparison with the samples with 2.5 mg L^{-1}, 10 mg L^{-1} and 20 mg L^{-1}, respectively. From day 3, the calculated concentration increased drastically, resulting in an overestimation of 252 % (8.8 ± 5.0 mg L^{-1}), 116 % (21.6 ± 9.7 mg L^{-1}) and 73 % (34.5 ± 10.5 mg L^{-1}), for the 2.5 mg L^{-1}, 10 mg L^{-1} and 20 mg L^{-1}, respectively. In the case of the dPADs stored in the fridge (Fig. 4**d**), for the 20 mg L^{-1} phosphate solution, the calculated concentration was 20.1 ± 1.8 mg L^{-1} (overestimation of 1 %) during the three weeks. For the 2.5 mg L^{-1} and 10 mg L^{-1} solutions, during the first 12 days the calculated overestimation was of 0 % (2.5 ± 0.1 mg L^{-1}) and 7 % (10.7 ± 0.8 mg L^{-1}). Nevertheless, from day 12–22, the error increased, with an overestimation of 108 % (5.2 ± 0.3 mg L^{-1}) and 21 % (12.1 ± 2.1 mg L^{-1}), in comparison to the 2.5 mg L^{-1} and 10 mg L^{-1} solutions, respectively. Therefore, if the dPADs need to be used after a longer time (*i.e.*, 12 days after their fabrication), they have to be stored at 4°C.

3.3. Optimization of the pH PAD

The design in Fig. S20a was used to study the effect of the pH in the range from 2 to 5.5 of the PBS reagent solution containing 0.01 mg mL^{-1} chlorophenol red and 10 wt% PDADMAC. The produces PADs were studied in two DIW-based solutions with an adjusted pH to 5.5 and 8.5. The results (Fig. S21**)** indicate that the optimal reagent pH should be 3.5 because produced the higher color contrast between the samples at pH 5.5 and 8.5.

The design in Fig. S20b was used with the optimized PBS reagent solution at pH 3.5 to study the analytical response of the PAD in the range of pH from 5 to 8.5. The intensity of the color changed for increasing pH, from yellow to purple (Fig. 5**a**), with a sensitivity of the plot representing the intensity against the pH of 0.043 ± 0.001 a.u. pH^{-1} in all the analyzed pH range (Fig. 5**b**), a coefficient of regression of 0.97 and reproducibility of the method fabrication (n = 5) with a relative standard deviation lower than 5 % for all the cases.

3.4. Characterization of the multiplexed PAD

The optimized individuals PADs for phosphate, nitrate and pH were integrated into a single device according to the design described in Section 2.3. Cross-talk between the different integrated PADs was investigated by modifying the one parameter (*i.e.*, phosphate, nitrate or pH) and keeping the other two constant.

No cross-talk was observed for all the assays. The measured phosphate (Fig. 6**a**), nitrate (Fig. 6**b**) and pH (Fig. 6**c**), did not interfere with the other parameters. Therefore, the proposed multiplexed PAD can be used for simultaneous detection of phosphate, nitrate and pH.

The filling speed of the channels for the nitrate and phosphate, and

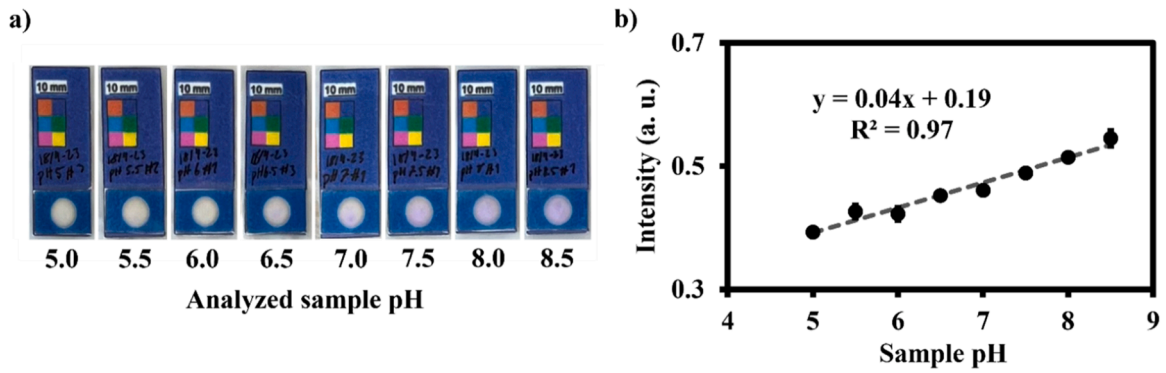

Fig. 5. Analytical response of the PAD for the pH detection. a) Photographs of the detection circles used for detecting the pH in the range from 5.0 to 8.5. b) Calibration plot of the measured intensity for each PAD against the pH of the analyzed solution. Errors represent the standard deviation for five replicates (n = 5).

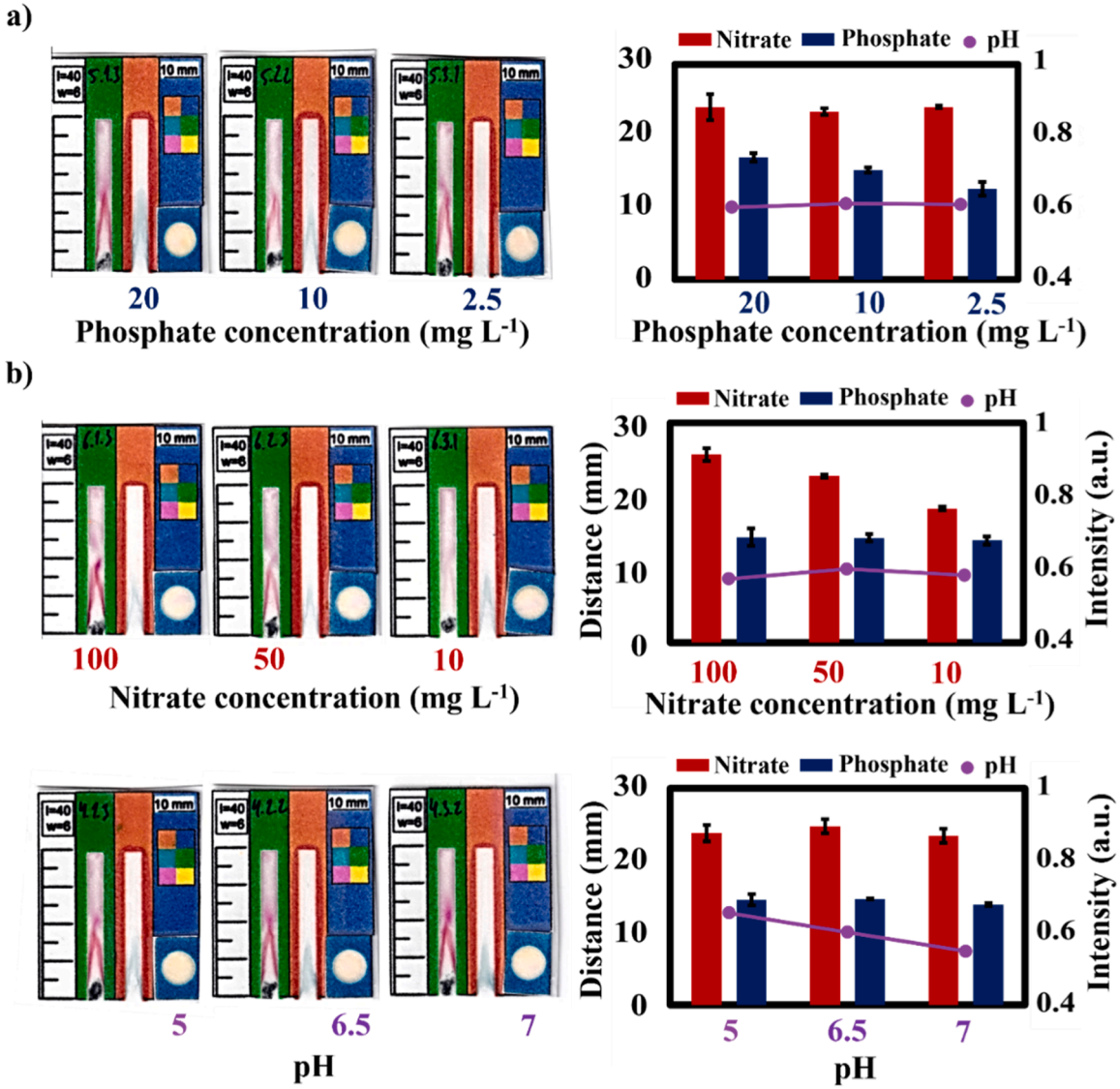

Fig. 6. Multiplexed analysis of the PAD. a) Cross-talk analysis changing the concentration of phosphate in the range from 2.5 to 20 mg L^{-1}, in the presence of 50 mg L^{-1} of nitrate at pH 7. b) Cross-talk analysis changing the concentration of nitrate in the range from 10 to 100 mg L^{-1}, in the presence of 10 mg L^{-1} of phosphate at pH 8. c) Cross-talk analysis changing the pH in the range from 5 to 7, in the presence of 50 mg L^{-1} of nitrate and 10 mg L^{-1} of phosphate. Error bars represent the standard deviation from five replicates (n = 5).

the time to keep a permanent intensity color change in the pH PAD was measured at different time points after dipping the multiplexed PAD in a water solution containing 20 mg L^{-1} of phosphate and 50 mg L^{-1} of nitrate at pH 7 (Fig. S22a). The results display a time of 12 min for filling both the nitrate and phosphate channels, as well as a sufficiently constant intensity of the pH after 1 min. Therefore, the multiplexed PAD needs to be dipped in the analysed solution for 12 min to obtain the colorimetric response for the three parameters. The change of response of each PAD was also analyzed at different time points during 60 min after removing the multiplexed PAD from the solution (Fig. S22b). The measured distance for the nitrate and phosphate did not change throughout the time analyzed, meanwhile the intensity measured for the pH slightly decreased (i.e., 10 % in relation to the original intensity) after 30 min, meaning that it would be better to take the images within 30 min after removing the multiplexed PAD from the solution to guarantee the good accuracy of detection.

3.5. Optimization of the soil extraction method

The cafetière-based extraction protocol was optimized using a commercial planting soil. Firstly, the effect of the waiting time after mixing the soil and the water (*i.e.*, extraction time) was checked (Fig. S23a), by pressing the piston 3 times and using 200 mL of water and 20 g of soil and waiting for 2 min, 3 min or 5 min. The calculated values for phosphate and nitrate are quite similar, with a lower standard deviation for 3 min (74.11 ± 0.45 mg L^{-1} and 12.73 ± 0.09 mg L^{-1}, for nitrate and phosphate, respectively), therefore this was selected as the best extraction time for the next assays. Secondly, the number of times that the piston is pressed for mixing the soil and the water was tested. The results in Fig. S23b show an increase of 11 % and 73 % for the calculated concentrations of nitrate and phosphate, respectively, when increasing the number of times from 2 to 5. For the tests with the piston pressed 5 times, the calculated concentrations were 76.22 ± 1.23 mg L^{-1} and 16.94 ± 0.88 mg L^{-1}, for nitrate and phosphate, respectively, and it was selected for the optimization of the other parameters. Then, the influence of the volume of water used as medium to extract the nutrients from soil was studied too (Fig. S23c). For 50 mL, the calculated concentrations were 7 % higher (85.12 ± 1.32 mg L^{-1}) and 30 % lower (14.34 ± 0.45 mg L^{-1}) than the expected concentrations in soil for nitrate and phosphate, respectively. For higher volumes, the calculated concentrations for nitrate (78.42 ± 0.45 mg L^{-1} and 76.21 ± 1.17 mg L^{-1}, for 200 mL and 300 mL, respectively) and phosphate (17.83 ± 0.09 mg L^{-1} and 16.92 ± 0.88 mg L^{-1}, for 200 mL and 300 mL, respectively) were slightly higher for the 200 mL with a lower standard deviation, therefore 200 mL was chosen as the optimal volume of water to extract the nutrients from soils. Finally, the influence of the mass of soil added to the cafetière was evaluated (Fig. S23d). From the results can be concluded that using 5 g of soil produces a worse extraction of both nutrients (65.53 ± 1.26 mg L^{-1} and 3.80 ± 0.44 mg L^{-1}, for nitrate and phosphate, respectively), but using 10 g of soil the extraction efficiency increases in relation to 20 g, being the calculated concentration of 79.62 ± 0.45 mg L^{-1} for nitrate and 20.10 ± 0.09 mg L^{-1} for phosphate, with an extraction efficiency of 100 % for both nutrients. Therefore, the optimal extraction was obtained by adding 10 g of soil and 200 mL of water, that were mixed pressing the plunger five times and keeping the mixed solution in the cafetière for 3 min before transferring it to a container for measuring the parameters with the multiplexed PAD.

3.6. Analysis of soil samples

The optimized protocol with the cafetière was applied to extract nutrients from four commercial soils and then, the optimized multiplexed PAD was used to analyze the concentration of the extracted phosphate, nitrate and the pH. The comparison between the calculated values with the multiplexed PAD and UV-Vis shows relative errors below 15 % (Table S7), except for soil 1, which had a relative error of 27 %, although with both standard deviations overlapping. The negative relative error for soil 2, soil 3 and soil 4 represents a slight underestimation of the calculated nitrate with the PAD in comparison to the UV-Vis. In case of the phosphate detection (Table S8), the relative error between the multiplexed PAD and the UV-Vis was below 14 %, except for soil 3 (50 %), but it is important to highlight that the concentration calculated from the UV-Vis is within the confidence interval of the calculated concentration by the PAD. For the pH detection, the values obtained from the PAD and the pH-meter show an excellent agreement (Table S9), with relative errors of 0 % for all the samples.

Comparing the values obtained from the multiplexed PAD with the labels of the soil packages, relative errors were below 14 % for all the soils for both nitrate (Table 1) and phosphate (Table 2). The positive relative errors represent a slight overestimation from the PAD, but all the labelled values were within the confidence interval from the PAD. For the pH (Table 3), the comparative study was also excellent, with relative errors of 0 % in all the cases, except for soil 4 (-17 %). This higher error is because the labelled pH value in the package is from 5 to 7, meaning that the calculated value from the PAD is within this interval, but the way for representing the data in the table causes this higher error.

Therefore, the excellent agreement between the calculated nitrate, phosphate and pH with the multiplexed PAD and the UV-Vis method, and specially with the values from the package labels demonstrates the feasible of the proposed method for a rapid and accurate analysis of nutrients in soils. It is also worth noting that the best comparative results were those obtained from the labelled values, which is the accredited composition by the brand.

4. Conclusions

A work-flow for monitoring soil nutrients (*i.e.*, nitrate, phosphate, pH) in less than 20 min has been developed using a cafetière-based method for extraction and a multiplexed PAD for detection. The extraction protocol for soil nutrients with the cafetière enables to extract 100 % of the nutrients from soils in 3 min, using 200 mL of DIW and 10 g of soil. The multiplexed PAD integrates two distance-based and one intensity-based readouts. The distance-based colorimetric readouts for phosphate and nitrate are based on the PMB reaction and on the Griess reaction integrated with a zinc reduction, respectively. Both dPADs show a high selectivity in the range 1.0 – 22.5 mg L^{-1} for phosphate and 10 – 100 mg L^{-1} for nitrate, in agreement with the concentration of the nutrients in soils. The intensity-based readout for pH is based on the use of the chlorophenol red indicator, giving a change in intensity in the pH range 5.0 – 8.5. The proposed method has been validated with commercial soils, comparing the results obtained with the multiplexed PAD with those obtained with the UV-Vis and those labelled on the soil packages. The comparative study showed a very good agreement, with overall relative errors below 14 %. The results demonstrate that this rapid and easy-to-use method developed here to monitor soil nutrients on-site will enable a more readily interpretation in the field in

Table 1
Values of nitrate concentration calculated with the multiplexed PAD and those labelled in the package for 4 soil samples. Errors represent the standard deviation for three different PADs fabricated under the same conditions (n = 3).

Sample	Calculated nitrate with the PAD (mg L^{-1})	Labelled nitrate in the package (mg L^{-1})	Relative error (%)(*)
Soil 1	57 ± 16	56	+2
Soil 2	87 ± 9	79	+10
Soil 3	87 ± 5	85	+2
Soil 4	67 ± 15	58	+14

(*) Positive and negative values indicate overestimation and underestimation, respectively, of the calculated nitrate concentration with the PAD in comparison to the labelled nitrate concentration in the package

Table 2
Values of phosphate concentration calculated with the multiplexed PAD and those labelled in the package for 4 soil samples. Errors represent the standard deviation for three different PADs fabricated under the same conditions (n = 3).

Sample	Calculated phosphate with the PAD (mg L^{-1})	Labelled phosphate in the package (mg L^{-1})	Relative error (%)(*)
Soil 1	8 ± 2	7	+14
Soil 2	8 ± 2	7	+14
Soil 3	3 ± 1	3	0
Soil 4	2 ± 0	2	0

* Positive and negative values indicate overestimation and underestimation, respectively, of the calculated phosphate concentration with the PAD in comparison to the labelled phosphate concentration in the package

Table 3
Values of pH calculated with the multiplexed PAD and those labelled in the package for 4 soil samples. Errors represent the standard deviation for three different PADs fabricated under the same conditions (n = 3).

Sample	Calculated pH with the PAD	Labelled pH in the package	Relative error (%)(*)
Soil 1	6 ± 1	6 ± 1	0
Soil 2	6 ± 0	6 ± 1	0
Soil 3	6 ± 0	6 ± 1	0
Soil 4	5 ± 0	6 ± 1	−17

* Positive and negative values indicate overestimation and underestimation, respectively, of the calculated pH with the PAD in comparison to the labelled pH in the package

comparison to current methods, resulting in a real impact of the developed work-flow to be applied on in-the-field analyses of multiple key soil nutrients by minimally trained operators in resource limited settings. Farmers in central Kenya have been testing protypes of the cafetière-based extraction method and several individual PADs to assess userfriendliness of the proposed workflow, and the study shows promising results [74].

CRediT authorship contribution statement

Pablo Gimenez-Gomez: Writing – review & editing, Writing – original draft, Visualization, Validation, Supervision, Methodology, Investigation, Formal analysis, Data curation, Conceptualization. **Nicolina Priem:** Methodology, Investigation, Formal analysis, Data curation. **Samantha Richardson:** Visualization, Conceptualization. **Nicole Pamme:** Writing – review & editing, Writing – original draft, Validation, Supervision, Resources, Project administration, Funding acquisition, Conceptualization.

Declaration of Competing Interest

The authors declare that they have no known competing financial interests or personal relationships that could have appeared to influence the work reported in this paper

Acknowledgments

This work was financially supported by the Carl Trygger Foundation (Project CTS21:1529). P. G.-G. is grateful to the European Union for the funding support received through the HORIZON-MSCA-2022-PF-01 actions (Project 101104159-DVD-E).

Appendix A. Supporting information

Supplementary data associated with this article can be found in the online version at doi:10.1016/j.snb.2024.136881.

Data Availability

Data will be made available on request.

References

[1] M. van Dijk, T. Morley, M.L. Rau, Y. Saghai, A meta-analysis of projected global food demand and population at risk of hunger for the period 2010–2050, Nat. Food 2 (2021) 494–501, https://doi.org/10.1038/s43016-021-00322-9.
[2] R. Davydov, M. Sokolov, W. Hogland, A. Glinushkin, A. Markaryan, The application of pesticides and mineral fertilizers in agriculture, MATEC Web Conf. (2018), https://doi.org/10.1051/matecconf/201824511003.
[3] W. Li, S. Guo, H. Liu, L. Zhai, H. Wang, Q. Lei, Comprehensive environmental impacts of fertilizer application vary among different crops: implications for the adjustment of agricultural structure aimed to reduce fertilizer use, Agric. Water Manag 210 (2018) 1–10, https://doi.org/10.1016/j.agwat.2018.07.044.
[4] S. Menegat, A. Ledo, R. Tirado, Greenhouse gas emissions from global production and use of nitrogen synthetic fertilisers in agriculture, Sci. Rep. 12 (2022), https://doi.org/10.1038/s41598-022-18773-w.
[5] H. Qin, K. Lu, P.J. Strong, Q. Xu, Q. Wu, Z. Xu, J. Xu, H. Wang, Long-term fertilizer application effects on the soil, root arbuscular mycorrhizal fungi and community composition in rotation agriculture, Appl. Soil Ecol. 89 (2015) 35–43, https://doi.org/10.1016/j.apsoil.2015.01.008.
[6] H. Rodríguez, R. Fraga, Phosphate solubilizing bacteria and their role in plant growth promotion, Biotechnol. Adv. 17 (1999) 319–339, https://doi.org/10.1016/S0734-9750(99)00014-2.
[7] N.M. Crawford, Nitrate: Nutrient and signal for plant growth, Plant Cell 7 (1995) 859–868.
[8] R.E. Lucas, J.F. Davis, Relationships between ph values of organic soils and availabilities of 12 plant nutrients, Soil Sci. 92 (1961) 177–182, https://doi.org/10.1097/00010694-196109000-00005.
[9] G.W. Thomas, 2018, Soil pH and soil acidity, 2018. https://doi.org/10.2136/sssabookser5.3.c16.
[10] S.H. Chien, L.I. Prochnow, S. Tu, C.S. Snyder, Agronomic and environmental aspects of phosphate fertilizers varying in source and solubility: an update review, Nutr. Cycl. Agroecosyst 89 (2011) 229–255, https://doi.org/10.1007/s10705-010-9390-4.
[11] W. Jiao, W. Chen, A.C. Chang, A.L. Page, Environmental risks of trace elements associated with long-term phosphate fertilizers applications: a review, Environ. Pollut. 168 (2012) 44–53, https://doi.org/10.1016/j.envpol.2012.03.052.
[12] C. Lu, H. Tian, Global nitrogen and phosphorus fertilizer use for agriculture production in the past half century: Shifted hot spots and nutrient imbalance, Earth Syst. Sci. Data 9 (2017) 181–192, https://doi.org/10.5194/essd-9-181-2017.
[13] R. Basosi, D. Spinelli, A. Fierro, S. Jez, Mineral nitrogen fertilizers: Environmental impact of production and use, 2014.
[14] M. Tayefeh, S.M. Sadeghi, S.A. Noorhosseini, J. Bacenetti, C.A. Damalas, Environmental impact of rice production based on nitrogen fertilizer use, Environ. Sci. Pollut. Res. 25 (2018) 15885–15895, https://doi.org/10.1007/s11356-018-1788-6.
[15] B.-M. Chen, Z.-H. Wang, S.-X. Li, G.-X. Wang, H.-X. Song, X.-N. Wang, Effects of nitrate supply on plant growth, nitrate accumulation, metabolic nitrate concentration and nitrate reductase activity in three leafy vegetables, Plant Sci. 167 (2004) 635–643, https://doi.org/10.1016/j.plantsci.2004.05.015.
[16] K. Mikula, G. Izydorczyk, D. Skrzypczak, M. Mironiuk, K. Moustakas, A. Witek-Krowiak, K. Chojnacka, Controlled release micronutrient fertilizers for precision agriculture – a review, Sci. Total Environ. 712 (2020), https://doi.org/10.1016/j.scitotenv.2019.136365.
[17] M. Calabi-Floody, J. Medina, C. Rumpel, L.M. Condron, M. Hernandez, M. Dumont, M.D.L.L. Mora, Smart Fertilizers as a Strategy for Sustainable Agriculture, 2018. https://doi.org/10.1016/bs.agron.2017.10.003.
[18] K. Lubkowski, Environmental impact of fertilizer use and slow release of mineral nutrients as a response to this challenge, Pol. J. Chem. Technol. 18 (2016) 72–79, https://doi.org/10.1515/pjct-2016-0012.
[19] World Health Organization. Regional Office for the Western Pacific, Sustainable development goals (SDGs): Goal 15: Protect, restore and promote sustainable use of terrestrial ecosystems, sustainably manage forests, combat desertification, and halt and reverse land degradation and halt biodiversity loss, WHO Regional Office for the Western Pacific (2016).
[20] C. Reimann, P. de Caritat, S. Albanese, M. Andersson, A. Arnoldussen, R. Baritz, M. J. Batista, A. Bel-lan, M. Birke, D. Cicchella, T. Wilson, A. Wygralak, New soil composition data for Europe and Australia: Demonstrating comparability, identifying continental-scale processes and learning lessons for global geochemical mapping, Sci. Total Environ. 416 (2012) 239–252, https://doi.org/10.1016/j.scitotenv.2011.11.019.
[21] P. Marschner, Z. Rengel, Nutrient availability in soils, Marschner's, Miner. Nutr. High. Plant.: Third Ed. (2012) 315–330, https://doi.org/10.1016/B978-0-12-384905-2.00012-1.
[22] Soil and Plant Analysis Council, in: Inc. (Ed.), Soil Analysis Handbook of Reference Methods, 1st ed., CRC Press, 1999.
[23] Y. Fan, X. Wang, T. Funk, I. Rashid, B. Herman, N. Bompoti, M.D.S. Mahmud, M. Chrysochoou, M. Yang, T.M. Vadas, Y. Lei, B. Li, A critical review for real-time continuous soil monitoring: advantages, challenges, and perspectives, Environ. Sci. Technol. 56 (2022) 13546–13564, https://doi.org/10.1021/acs.est.2c03562.

[24] N. Pourreza, H. Sharifi, H. Golmohammadi, A green chemosensor for colorimetric determination of phosphate ion in soil, bone, and water samples using curcumin nanoparticles, Anal. Sci. 36 (2020) 1297–1302, https://doi.org/10.2116/analsci.20P101.
[25] T.M.S. Sattolo, R. Otto, E. Mariano, M.Y. Kamogawa, Adaptation and validation of colorimetric methods in determining ammonium and nitrate on tropical soils, Commun. Soil Sci. Plant Anal. 47 (2016) 2547–2557, https://doi.org/10.1080/00103624.2016.1243710.
[26] A.S. Baker, Colorimetric determination of nitrate in soil and plant extracts with brucine, J. Agric. Food Chem. 15 (1967) 802–806, https://doi.org/10.1021/jf60153a004.
[27] T.A. Doane, W.R. Horwáth, Spectrophotometric determination of nitrate with a single reagent, Anal. Lett. 36 (2003) 2713–2722, https://doi.org/10.1081/AL-120024647.
[28] A. Verma, B.D. Gupta, Fiber optic surface plasmon resonance based disposable probe for the detection of phosphate ion in soil, Opt. (Stuttg.) 243 (2021), https://doi.org/10.1016/j.ijleo.2021.167484.
[29] S. Ganesh, F. Khan, M.K. Ahmed, P. Velavendan, N.K. Pandey, U. Kamachi Mudali, Spectrophotometric determination of trace amounts of phosphate in water and soil, Water Sci. Technol. 66 (2012) 2653–2658, https://doi.org/10.2166/wst.2012.468.
[30] P. Das, B. Chetry, S. Paul, S.S. Bhattacharya, P. Nath, Detection and quantification of phosphate in water and soil using a smartphone, Microchem. J. 172 (2022), https://doi.org/10.1016/j.microc.2021.106949.
[31] N. Moonrungsee, S. Pencharee, J. Jakmunee, Colorimetric analyzer based on mobile phone camera for determination of available phosphorus in soil, Talanta 136 (2015) 204–209, https://doi.org/10.1016/j.talanta.2015.01.024.
[32] V. Lavanya, A. Nayak, S. Dasgupta, S. Urkude, S. Dey, A. Biswas, B. Li, D. C. Weindorf, S. Chakraborty, A smartphone-integrated imaging device for measuring nitrate and phosphate in soil and water samples, Microchem. J. 193 (2023), https://doi.org/10.1016/j.microc.2023.109042.
[33] O. Benslimane, R. Rabie, S. El Hajjaji, The Use of ISFET for the Measurement of Phosphorus in Moroccan Soils, 2023. https://doi.org/10.1007/978-3-031-35248-5_41.
[34] S.R. Burge, K.D. Hristovski, R.G. Burge, D. Saboe, D.A. Hoffman, S.S. Koenigsberg, Microbial potentiometric sensor array measurements in unsaturated soils, Sci. Total Environ. 751 (2021), https://doi.org/10.1016/j.scitotenv.2020.142342.
[35] S. Dudala, S.K. Dubey, S. Goel, Microfluidic soil nutrient detection system: integrating nitrite, pH, and electrical conductivity detection, IEEE Sens J. 20 (2020) 4504–4511, https://doi.org/10.1109/JSEN.2020.2964174.
[36] V.O. Ebuele, D.G. Congrave, C.D. Gwenin, V. Fitzsimmons-Thoss, Development of a cobalt electrode for the determination of phosphate in soil extracts and comparison with standard methods, Anal. Lett. 51 (2018) 834–848, https://doi.org/10.1080/00032719.2017.1360899.
[37] S.J. Birrell, J.W. Hummel, Membrane selection and ISFET configuration evaluation for soil nitrate sensing, Trans. Am. Soc. Agric. Eng. 43 (2000) 197–206.
[38] G. Archbold, C. Parra, H. Carrillo, A.M. Mouazen, Towards the implementation of ISFET sensors for in-situ and real-time chemical analyses in soils: a practical review, Comput. Electron Agric. 209 (2023), https://doi.org/10.1016/j.compag.2023.107828.
[39] C.L. Baumbauer, P.J. Goodrich, M.E. Payne, T. Anthony, C. Beckstoffer, A. Toor, W. Silver, A.C. Arias, Printed potentiometric nitrate sensors for use in soil, Sensors 22 (2022), https://doi.org/10.3390/s22114095.
[40] M. Ramesh, D.K. Kharbanda, S. Kumar, D. Kumar, P.K. Khanna, N. Suri, Potentiometric testing of soil by printed nobel metal thick film electrode, J. Electrochem Soc. 170 (2023), https://doi.org/10.1149/1945-7111/acb5c8.
[41] M. Kundu, P. Krishnan, K.A. Chobhe, K.M. Manjaiah, R.P. Pant, G. Chawla, Fabrication of electrochemical nanosensor for detection of nitrate content in soil extract, J. Soil Sci. Plant Nutr. 22 (2022) 2777–2792, https://doi.org/10.1007/s42729-022-00845-5.
[42] S. Chen, J. Chen, M. Qian, J. Liu, Y. Fang, Low cost, portable voltammetric sensors for rapid detection of nitrate in soil, Electro Acta 446 (2023), https://doi.org/10.1016/j.electacta.2023.142077.
[43] Agriculture test kit,HI3896, (n.d.). ⟨https://hannainst.com.au/hi3896-hanna-soil-test-kit⟩ (accessed September 22, 2023).
[44] Luster Leaf: Digital Soil Test Kit, (n.d.). ⟨http://www.lusterleaf.com/nav/soil_test.html⟩ (accessed September 22, 2023).
[45] Refill for Rapitest® Soil Test Kit, (n.d.). ⟨https://www.flinnsci.com/soil-test-refill-kit—rapitest/fb0427/⟩ (accessed September 22, 2023).
[46] Soil Analyzer Model RS-TRREC-N01-1, (n.d.). ⟨https://www.renkeer.com/product/portable-soil-analyzer/⟩ (accessed September 22, 2023).
[47] P. Aryal, C. Hefner, B. Martinez, C.S. Henry, Microfluidics in environmental analysis: advancements, challenges, and future prospects for rapid and efficient monitoring, Lab Chip 24 (2024) 1175–1206, https://doi.org/10.1039/d3lc00871a.
[48] A. Pal, S.K. Dubey, S. Goel, IoT enabled microfluidic colorimetric detection platform for continuous monitoring of nitrite and phosphate in soil, Comput. Electron Agric. 195 (2022), https://doi.org/10.1016/j.compag.2022.106856.
[49] Y. Li, Q. Yang, M. Chen, M. Wang, M. Zhang, An ISE-based on-site soil nitrate nitrogen detection system, Sens. (Switz.) 19 (2019), https://doi.org/10.3390/s19214669.
[50] M.A. Ali, K. Mondal, Y. Wang, N.K. Mahal, M.J. Castellano, L. Dong, Microfluidic detection of soil nitrate ions using novel electrochemical foam electrode, in: Proceedings of the IEEE International Conference on Micro Electro Mechanical Systems (MEMS), 2017: pp. 482–485. https://doi.org/10.1109/MEMSYS.2017.7863448.
[51] H. Zhang, R. Zhao, Y. Yang, Y. Liu, L. Han, Measuring nitrate concentration in surface waters with a microfluidic device facilitated by a miniaturized capacitive deionization cell, Water Qual. Res. J. 58 (2023), https://doi.org/10.2166/wqrj.2023.010.
[52] S. Dudala, S.K. Dubey, S. Goel, Microfluidic soil nutrient detection system: integrating nitrite, pH, and electrical conductivity detection, IEEE Sens J. 20 (2020) 4504–4511, https://doi.org/10.1109/JSEN.2020.2964174.
[53] E. Noviana, T. Ozer, C.S. Carrell, J.S. Link, C. McMahon, I. Jang, C.S. Henry, Microfluidic paper-based analytical devices: from design to applications, Chem. Rev. 121 (2021) 11835–11885, https://doi.org/10.1021/acs.chemrev.0c01335.
[54] T. Thongkam, K. Hemavibool, An environmentally friendly microfluidic paper-based analytical device for simultaneous colorimetric detection of nitrite and nitrate in food products, Microchem. J. 159 (2020), https://doi.org/10.1016/j.microc.2020.105412.
[55] M.I. Umeda, K. Danchana, T. Fujii, E. Hino, Y. Date, K. Aoki, T. Kaneta, Reduction with zinc — impact on the determination of nitrite and nitrate ions using microfluidic paper-based analytical devices, Talanta Open 10 (2024), https://doi.org/10.1016/j.talo.2024.100347.
[56] B.M. Jayawardane, S. Wei, I.D. McKelvie, S.D. Kolev, Microfluidic paper-based analytical device for the determination of nitrite and nitrate, Anal. Chem. 86 (2014) 7274–7279, https://doi.org/10.1021/ac5013249.
[57] B. Waghwani, S. Balpande, J. Kalambe, Development of microfluidic paper based analytical device for detection of phosphate in water, Int. J. Innov. Technol. Explor. Eng. 8 (2019) 592–595.
[58] S. Richardson, A. Iles, J.M. Rotchell, T. Charlson, A. Hanson, M. Lorch, N. Pamme, Citizen-led sampling to monitor phosphate levels in freshwater environments using a simple paper microfluidic device, PLoS One 16 (2021), https://doi.org/10.1371/journal.pone.0260102.
[59] A. Manbohi, S.H. Ahmadi, Portable smartphone-based colorimetric system for simultaneous on-site microfluidic paper-based determination and mapping of phosphate, nitrite and silicate in coastal waters, Environ. Monit. Assess. 194 (2022), https://doi.org/10.1007/s10661-022-09860-6.
[60] R. Catalan-Carrio, J. Saez, L.Á. Fernández Cuadrado, G. Arana, L. Basabe-Desmonts, F. Benito-Lopez, Ionogel-based hybrid polymer-paper handheld platform for nitrite and nitrate determination in water samples, Anal. Chim. Acta 1205 (2022), https://doi.org/10.1016/j.aca.2022.339753.
[61] L. Merino, Development and validation of a method for determination of residual nitrite/nitrate in foodstuffs and water after zinc reduction, Food Anal. Methods 2 (2009) 212–220, https://doi.org/10.1007/s12161-008-9052-1.
[62] S.R. Crouch, H.V. Malmstadt, A mechanistic investigation of molybdenum blue method for determination of phosphate, Anal. Chem. 39 (1967) 1084–1089, https://doi.org/10.1021/ac60254a027.
[63] D.M. Cate, W. Dungchai, J.C. Cunningham, J. Volckens, C.S. Henry, Simple, distance-based measurement for paper analytical devices, Lab Chip 13 (2013) 2397–2404, https://doi.org/10.1039/c3lc50072a.
[64] G. Singh, G. Kaur, K. Williard, J. Schoonover, J. Kang, Monitoring of water and solute transport in the vadose zone: A review, Vadose Zone J. 17 (2018), https://doi.org/10.2136/vzj2016.07.0058.
[65] A. Charbaji, H. Heidari-Bafroui, C. Anagnostopoulos, M. Faghri, A new paper-based microfluidic device for improved detection of nitrate in water, Sens. (Switz.) 21 (2021) 1–15, https://doi.org/10.3390/s21010102.
[66] N. Lopez-Ruiz, V.F. Curto, M.M. Erenas, F. Benito-Lopez, D. Diamond, A.J. Palma, L.F. Capitan-Vallvey, Smartphone-based simultaneous pH and nitrite colorimetric determination for paper microfluidic devices, Anal. Chem. 86 (2014) 9554–9562, https://doi.org/10.1021/ac5019205.
[67] M.J. Moorcroft, J. Davis, R.G. Compton, Detection and determination of nitrate and nitrite: a review, Talanta 54 (2001) 785–803, https://doi.org/10.1016/S0039-9140(01)00323-X.
[68] E.A. Nagul, I.D. McKelvie, P. Worsfold, S.D. Kolev, The molybdenum blue reaction for the determination of orthophosphate revisited: opening the black box, Anal. Chim. Acta 890 (2015) 60–82, https://doi.org/10.1016/j.aca.2015.07.030.
[69] G.D. Christian, P.K. Dasgupta, K.A. Schug. Analytical Chemistry, 7th ed., Wiley, 2013.
[70] P. Giménez-Gómez, I. Hättestrand, S. Sjöberg, C. Dupraz, S. Richardson, N. Pamme, Distance-based paper analytical device for the determination of dissolved inorganic carbon concentration in freshwater, Sens Actuators B Chem. 385 (2023), https://doi.org/10.1016/j.snb.2023.133694.
[71] J.L. Chen, D.I. Njoku, C. Tang, Y. Gao, J. Chen, Y.-K. Peng, H. Sun, G. Mao, M. Pan, N.F.-Y. Tam, Advances in microfluidic paper-based analytical devices (μPADs): design, fabrication, and applications, Small Methods (2024), https://doi.org/10.1002/smtd.202400155.
[72] M.K. Seikel, Oxidation products of sulfanilamide, J. Am. Chem. Soc. 62 (1940) 1214–1216, https://doi.org/10.1021/ja01862a065.
[73] J. Murphy, J.P. Riley, A modified single solution method for the determination of phosphate in natural waters, Anal. Chim. Acta 27 (1962) 31–36, https://doi.org/10.1016/S0003-2670(00)88444-5.
[74] P. Kamau, I. Ndirangu, S. Richardson, N. Pamme, J. Gitaka, Gendered farmer perceptions towards soil nutrition and willingness to pay for a cafetiere-style filter system for soil testing in situ: evidence from Central Kenya, Heliyon 10 (2024). https://doi.org/10.1016/j.heliyon.2024.e37568.

Dr. Pablo Gimenez-Gomez, researcher (Marie Skłodowska-Curie Actions Fellow) at Stockholm University. He has long experience in the development of lab-on-a-chip systems that combine optical and electrochemical sensors with microfluidic architectures applied to the detection of analytes of interest in the food/beverage industry, environmental control or clinical diagnostics. He has participated in 9 national projects (one as PI), 2 international projects (as PI) and 7 R&D Innovation Contracts (three as PI). He is scientific advisor of The Smart Lollipop, a technological start-up working in the development of

point-of-care clinical devices. He has published 32 peer-reviewed papers, he is co-author of 1 patent and he has also presented more than 35 works at scientific conferences in those fields, 1 for invitation.

Mrs. Nicolina Priem obtained the Bachelor's degree in Chesmistry (2023) from the Stockholm University. At the present, she is a master student (Analytical Chemistry) at the Stockholm University.

Dr. Samantha Richardson is an early career researcher and lecturer at the University of Hull. She obtained her PhD in analytical chemistry in 2021 from the University of Hull. She has experience of environmental analysis and developing lab on a chip sensors for environmental applications. She has worked on a number of national and international research and knowledge exchange projects.

Prof Nicole Pamme, Professor in Analytical at Stockholm University and a Visiting Professor at the University of Hull (UK). She is an internationally leading expert with +20 years of experience in the design and fabrication of lab-on-a-chip devices, with a particular focus on chip-based bioassays. She is a Fellow of the Royal Society of Chemistry (FRSC) and the Higher Education Academy (FHEA). Nicole is an Associate Editor for Analyst (RSC) and on the Editorial Advisory Boards of Analytica Chimica Acta (Elsevier) and Lab on a Chip (RSC). She is included in the Analytical Scientist 2021 Power List of the world's most influential analytical scientists. She served on the Board of the Chemical and Biological Microsystems Society (CBMS), including as its President (2019–21). She was co-awarded the Newton Country Prize for Kenya (2020) for her work on point-of-care diagnostics for maternal health. She has +150 publications (+7000 citations, h-index 35) and has secured +€5.4 M in research funding.